Cell Reports
Report

Type III Effector VopC Mediates Invasion for *Vibrio* Species

Lingling Zhang,[1] Anne Marie Krachler,[1] Christopher A. Broberg,[1,5] Yan Li,[2] Hamid Mirzaei,[2] Christopher J. Gilpin,[3] and Kim Orth[1,4,*]
[1]Department of Molecular Biology
[2]Protein Chemistry Technology Center
[3]Department of Cell Biology
[4]Department of Biochemistry
UT Southwestern Medical Center, Dallas, TX 75390, USA
[5]Present address: Department of Genetics, The University of North Carolina, Chapel Hill, NC 27599-7290, USA
*Correspondence: kim.orth@utsouthwestern.edu
DOI 10.1016/j.celrep.2012.04.004

SUMMARY

Vibrio **spp. are associated with infections caused by contaminated food and water. A type III secretion system (T3SS2) is a shared feature of all clinical isolates of *V. parahaemolyticus* and some *V. cholerae* strains. Despite its being responsible for enterotoxicity, no molecular mechanism has been determined for the T3SS2-dependent pathogenicity. Here, we show that although *Vibrio* spp. are typically thought of as extracellular pathogens, the T3SS2 of *Vibrio* mediates host cell invasion, vacuole formation, and replication of intracellular bacteria. The catalytically active effector VopC is critical for *Vibrio* T3SS2-mediated invasion. There are other marine bacteria encoding VopC homologs associated with a T3SS; therefore, we predict that these bacteria are also likely to use T3SS-mediated invasion as part of their pathogenesis mechanisms. These findings suggest a new molecular paradigm for *Vibrio* pathogenicity and modify our view of the roles of T3SS effectors that are translocated during infection.**

INTRODUCTION

A type III secretion system (T3SS) is used by bacterial pathogens to inject effector proteins into the cytoplasm of their host cells. While the T3SS machinery is often conserved among Gram-negative pathogens, the effectors from each system differ widely in their mechanism of action. These effectors are typically potent proteins that mimic or capture an endogenous eukaryotic activity to disrupt the cellular response to infection (Broberg and Orth, 2010; Ham et al., 2011). Comparative genome analysis has demonstrated that a common *Vibrio* progenitor gave rise to *V. parahaemolyticus*, *V. cholerae*, and other *Vibrio* species (Okada et al., 2009). The acquisition of a T3SS similar to that found in *Yersinia* species (causal agent of the Plague and gastroenteritous), herein referred to as T3SS1, is one of the distinguishing features between *V. parahaemolyticus* and *V. cholerae* (Okada et al., 2010a).

The more recent acquisitions by *V. parahaemolyticus* of a second type III secretion system (T3SS2), thermostable direct hemolysins (TdhA/S) and TDH related hemolysin (TRH), have given rise to a diverse set of pathogenic strains, enabling the bacteria to adapt a host-associated lifestyle (Makino et al., 2003; Nishibuchi and Kaper, 1995). T3SS2 is located on a pathogenicity island that is hypothesized to be encoded on a mobile genetic element and is a shared feature of all characterized clinical isolates of *V. parahaemolyticus* and some *V. cholerae* strains (Okada et al., 2010b). Despite its discovery more than sixty years ago and suggestions that some *V. parahaemolyticus* strains are invasive, no molecular mechanism has been determined for the pathogenicity linked to clinical presentation of gastroenteritis (Akeda et al., 1997; Broberg et al., 2011; Makino et al., 2003). Herein, we have discovered that the enterotoxic T3SS2 mediates invasion of *V. parahaemolyticus* into nonphagocytic cells using an effector, VopC (Park et al., 2004a). This mechanism also appears to be shared by some epidemic *V. cholerae* non-O1 strains that do not contain cholera toxin. This VopC-containing T3SS is found in a number of marine bacteria, suggesting a previously uncharacterized pathogenesis mechanism for these bacterial pathogens.

RESULTS

T3SS2 of *V. parahaemolyticus* Mediates Bacterial Invasion into Nonphagocytic Host Cells

On the basis of G-C content, the T3SS1 of *V. parahaemolyticus* was ancestrally acquired, while the clinically associated T3SS2 was obtained through a relatively recent lateral gene transfer of a pathogenicity island (Makino et al., 2003). Although the evolutionary history of *V. parahaemolyticus* subsequently diverged from that of *V. cholerae*, in which some strains acquired either a T3SS2 or a phage-encoded cholera toxin, respectively, the two species contain remarkable similar T3SS2s and the effectors associated with this secretion system are well conserved (Okada et al., 2010b). Among known T3SS2 effectors, there is VopC (VPA1321 in *V. parahaemolyticus* RIMD2210633), which shows sequence similarity to the catalytic domain of cytotoxic necrotizing factor (CNF) toxins, including those secreted by *Yersinia* spp., *Bordetella* spp., and *Escherichia coli* (Table S1). *V. parahaemolyticus* appears to have hijacked the catalytic

domain from the toxins, since VopC encodes for a T3SS2 secretion signal linked to that enzymatic domain. By contrast, the toxins must encode distinct domains for them to be secreted by bacteria, to be taken up by the host cells, and to modify host cell targets. These toxins induce changes in cell shape and facilitate invasion of the pathogens into the host cell (Aktories and Barbieri, 2005). Therefore, it is logical to ask whether *Vibrio* T3SS2 uses VopC to mediate bacterial invasion into a host cell.

Our studies into the role of the *V. parahaemolyticus* T3SS2 and initial examination of *Vibrio* invasion involve the CAB2 strain, derived from the pathogenic RIMD strain. CAB2 contains an active T3SS2 but does not express the hemolysins and T3SS1, which allows for T3SS2 activity to be studied independently of other virulence factors. As a control we used the CAB4 strain, which does not contain active hemolysins, T3SS1 or T3SS2 (Table S2). Initial infection and cytotoxicity assays demonstrated that CAB2 induced with bile salt was able to cause changes in cell shape, followed by cell lysis approximately 4–5 hr after infection (Gotoh et al., 2010) (Figures 1A–1D). Surprisingly, our observations also suggested that the T3SS2-only CAB2 was invading host cells. When invasion of nonphagocytic HeLa cells was analyzed over time, the amount of intracellular CAB2 increased in the first few hours of infection and then precipitously dropped at approximately 4–5 hr, coincident with the timing of cell lysis (Figure 1E). The numbers of intracellular bacteria over time after initial infection were also quantitated by incubating the infected cells in medium containing gentamicin to kill extracellular bacteria and eliminate the possibility of reinfection. An increase in the number of surviving (intracellular) bacteria, followed by a dramatic decrease coincident with cell lysis at the end of the time course, suggests that *Vibrio* was able to replicate inside host cells (Figure 1F). The invasion efficiency of CAB2 was comparable to that of the intracellular pathogen *Shigella flexneri* (Figure 1G), and we observed similar results with differentiated epithelial colorectal CaCo2 cells (Figure S1). These studies support the hypothesis that *V. parahaemolyticus* uses a T3SS2-mediated mechanism for invasion, intracellular replication, and lysis of infected cells and is consistent with an early, isolated observation for a few invasive pathogenic *V. parahaemolyticus* strains (Akeda et al., 1997).

To further characterize host cell invasion, we analyzed HeLa cells infected with the same *V. parahaemolyticus* strains by transmission electron microscopy (TEM). HeLa cells infected with CAB2, but not CAB4, contained intracellular bacteria (Figures 1H and 1I).

The T3SS2 Effector VopC Promotes *Vibrio* Invasion by Activating Rac and CDC42

Next, we investigated the role of VopC in T3SS2-mediated invasion. The catalytic domain shared by VopC and the CNF toxins is predicted to have deamidase/transglutaminase activity that has been associated with modification of Rho family GTPases, including Rac, Rho, and/or CDC42 (Flatau et al., 1997). The conserved catalytic residues in VopC are cysteine 220 and histidine 235 (866 and 881 in CNF1, respectively) (Figure 2A). Modified by toxins CNF or DNT (*Bordetella* dermonecrotizing toxin) through deamidation or transglutamination, respectively, a Rho GTPase becomes constitutively active, triggering changes in the actin cytoskeleton of the infected cell (Masuda et al., 2000; Schmidt et al., 1997). These changes in cell shape facilitate invasion of the pathogens into the host cell (Doye et al., 2002).

Therefore, we tested whether *Vibrio* invasion was dependent on the presence of VopC. CAB2 and CAB2Δ*vopC*+VopC, but not CAB2Δ*vopC*, were able to invade HeLa cells (Figures 2B–2D), suggesting a critical role for VopC in invasion. While VopC is necessary for invasion, the cytotoxicity of T3SS2 is independent of VopC and is most likely due to the delivery of other effectors (Figures S2A and S2B). To assess whether the enzymatic activity of VopC was critical, we analyzed invasion mediated by the VopC deletion strain complemented with the putative catalytically inactive VopC C220S. In contrast to the CAB2Δ*vopC*+VopC strain, the CAB2Δ*vopC*+VopC C220S strain was unable to mediate invasion (Figure 2B), while VopC C220S was expressed and secreted at a level similar to that of wild-type VopC (Figure S2C). Cytoskeletal inhibitors were reported to be able to block invasive *V. parahaemolyticus* (Akeda et al., 1997). In the presence of inhibitors nocodazole or cytochalasin D, CAB2 was indeed no longer invasive, supporting the hypothesis that VopC induces changes in cytoskeleton shape to facilitate invasion (Figure 2B). To further investigate the invasion process, we analyzed HeLa cells infected with various strains by TEM. HeLa cells infected with CAB2Δ*vopC*+VopC, but not CAB2Δ*vopC*, contained intracellular bacteria (Figures 2C and 2D). The number of intracellular bacteria varied, and in some cases, intracellular bacteria appeared to be replicating (Figure 2C).

Next, we assessed whether VopC uses a mechanism similar to CNF toxins by analyzing the active state of host GTPases. Over the course of infection with CAB2, but not with CAB2Δ*vopC,* CDC42 was activated, as demonstrated by its interaction with its downstream target, the binding domain of p21-activated kinase 3 (PAK PBD) (Figure 3A). Infections with a deletion strain reconstituted with wild-type VopC (CAB2Δ*vopC*+VopC), but not with the deletion strain reconstituted with a putative catalytically inactive VopC (CAB2Δ*vopC*+VopC C220S), also caused CDC42 activation without affecting the total level of this GTPase (Figure 3A). These studies implicate the catalytic activity of VopC in the activation of Rho GTPases during infection.

To further test the activity of VopC, we transfected HeLa cells with VopCΔ67, an N-terminal truncation that retains the catalytic domain but removes the putative signal sequence to aid expression. Transfection of HeLa cells with VopCΔ67, but not GFP or VopCΔ67 C220S, induced the formation of both actin ruffles and filopodia (Figures 3B–3G). These changes in cell morphology appeared to be due to the enzymatic activity of VopC, because transfection of the predicted catalytically inactive VopCΔ67 C220S did not induce changes in the actin cytoskeleton when the proteins were expressed at a similar level in HeLa cells (Figure S3A).

Further biochemical analysis of the transfected cells revealed that the expression of VopCΔ67, but not VopCΔ67 C220S, caused the activation of both Rac and CDC42, but not RhoA, as measured by the ability of the activated GTPases to interact with their downstream targets, PAK PBD or the binding domain of Rhotekin, respectively (Figure 3H). The specificity of VopC for Rac and CDC42 but not RhoA is distinct from the activities

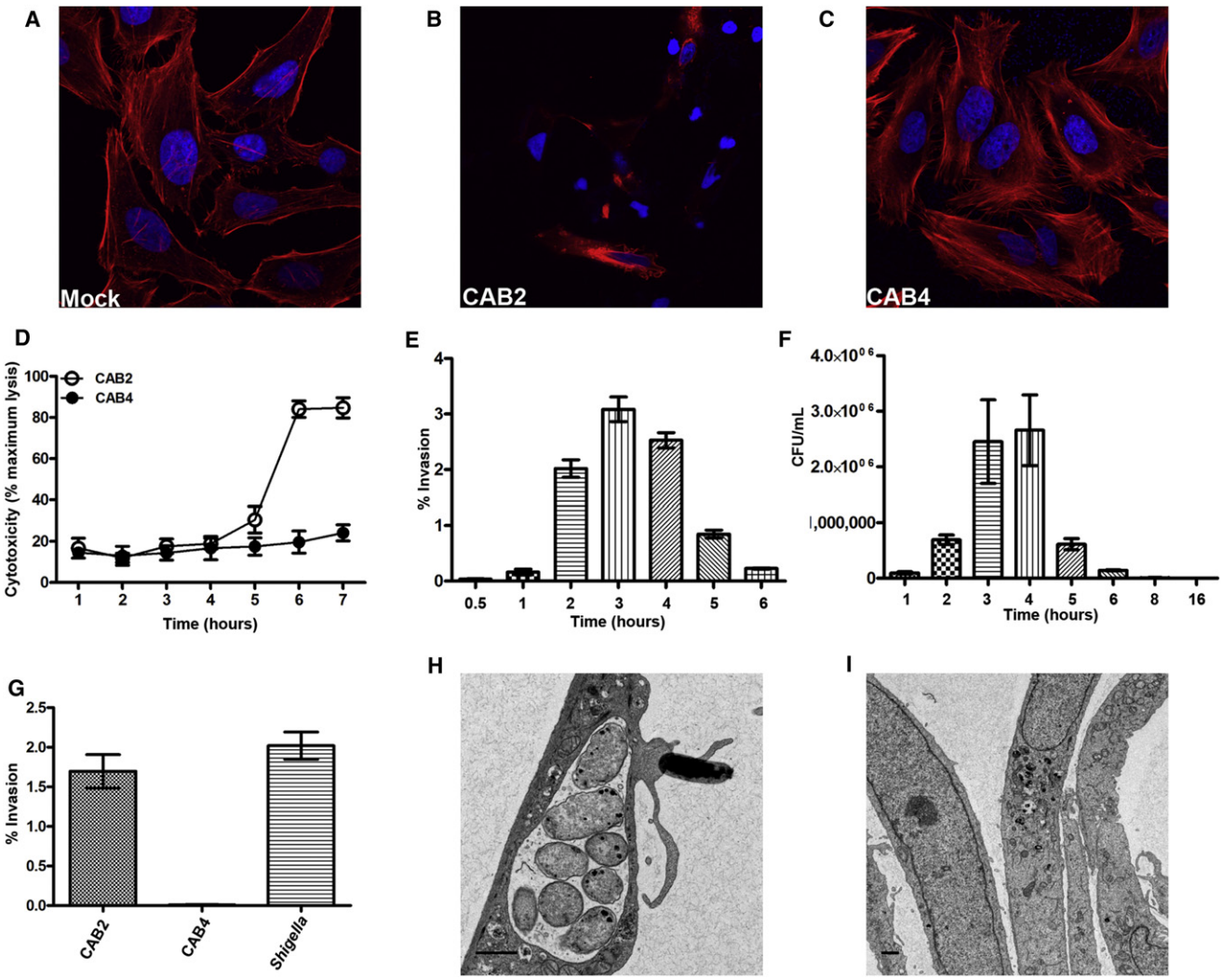

Figure 1. *V. parahaemolyticus* Invasion into HeLa Cells

(A–C) HeLa cells uninfected and infected with CAB2 or CAB4 after 5 hr, respectively. Nuclei were stained with Hoechst (blue), and the actin cytoskeleton was stained with rhodamine-phalloidin (red).

(D) HeLa cells infected with CAB2 (open circles) or CAB4 (closed circles) and LDH release evaluated to measure cytotoxicity. Error bars represent mean ± SD (n = 3).

(E) HeLa cells infected with CAB2. Invasion percentages were determined at indicated time points. Results are calculated from the numbers of intracellular bacteria collected per the numbers of total bacteria incubated in the same condition at indicated time points. Error bars represent mean ± SD (n = 3).

(F) HeLa cells were infected with CAB2 for 2 hr and incubated in medium containing gentamicin. The intracellular bacteria were determined at the indicated time points. Error bars represent mean ± SD (n = 3).

(G) HeLa cells were infected with CAB2, CAB4, or *Shigella* for 2 hr, and invasion percentages were determined. Results are calculated from the numbers of intracellular bacteria collected per the number of total bacteria. Error bars represent mean ± SD (n = 3).

(H and I) HeLa cells infected with CAB2 and CAB4, respectively. Scale bar represents 1 μm.

observed with the secreted CNF toxins, where CNF1 and DNT activate Rac, CDC42, and RhoA by deamidation and/or transglutamination (Horiguchi, 2001).

The T3SS2 Effector VopC Activates Rac by Deamidation of Glutamine 61

To test the biochemical activities of VopC, we first performed a transglutamination assay using the fluorescent amine-donor dansylcadaverine and Rho GTPases as substrates. MBP-VopCΔ67, but not MBP-VopCΔ67 C220S, was able to transglutaminate Rac and CDC42, but not RhoA with dansylcadaverine, which is consistent with the selective activation of these GTPases observed during transfection (Figures 3H and 3I, Figure S3B). CNF1 and DNT toxins modify Q61 in the switch 2 region of Rac and CDC42, resulting in constitutive activation of these small G proteins (Aktories and Barbieri, 2005). We observed that VopC was unable to transglutaminate a Rac Q61L mutant, supporting the hypothesis that VopC also targets

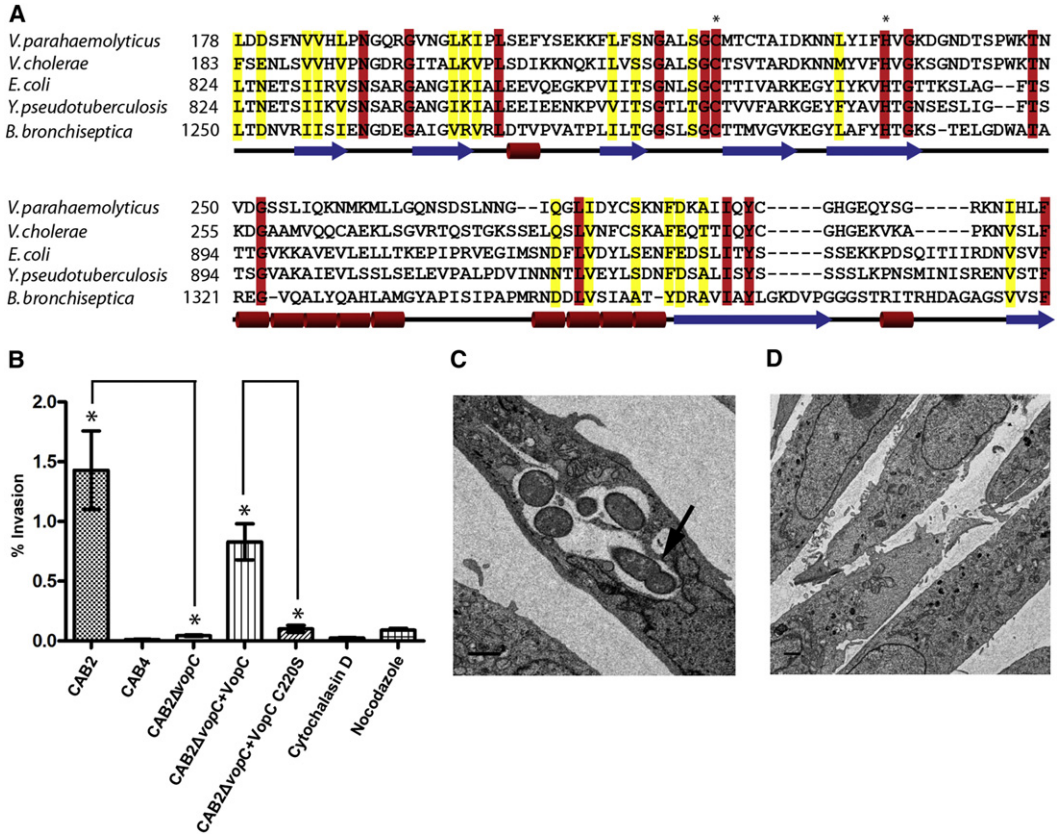

Figure 2. VopC Promotes *Vibrio* Invasion by Activating Rac and CDC42

(A) Multiple sequence alignment of VopC effectors and CNF and DNT toxins. Sequences are labeled according to species and residue numbers left of the alignment. Conserved residues are shown in yellow (similar) and red (identical). Conserved catalytic residues are marked by an asterisk. Secondary structure elements indicated are based on the structure of the catalytic domain of *E. coli* CNF1 (PDB 1HQ0) (SS: red cylinder α-helix; blue arrow: β strand). Alignments are shown for VopC (VPA1321), VopC (A55_B0294), CNF1 (UTI89_C4921), CNFY (YPK_2615), and DNT (BB3978).

(B) HeLa cells infected with CAB2, CAB4, CAB2Δ*vopC*, CAB2Δ*vopC* + VopC, CAB2Δ*vopC* + VopC C220S, or CAB2 in the presence of cytochalasin D or nocodazole. Error bars represent mean ± SD (n = 3). Asterisks indicate statistically significant differences between intracellular CAB2 and CAB2Δ*vopC* ($p = 0.0003$, n = 3) and between intracellular CAB2Δ*vopC* + VopC and CAB2Δ*vopC* + VopC C220S ($p = 0.0004$, n = 3), with the use of a two-tailed t test.

(C and D) HeLa cells infected with CAB2Δ*vopC* + VopC or CAB2Δ*vopC*. Arrow indicates replicating bacterium inside a HeLa cell. Scale bar represents 1μm.

this residue specifically (Figure 3I). We further observed that MBP-VopCΔ67, but not MBP-VopCΔ67 C220S, could also act as a deamidase. Ammonia release resulting from a deamidation reaction was detected when VopC was incubated with Rac, but not Rac Q61L, further suggesting that Q61 is the target residue of VopC activity (Figure 3J). To confirm the activity and residue specificity that VopC exerts on Rho family GTPases, we expressed GST-Rac in the presence or absence of MBP-VopCΔ67 and determined the total mass of purified GST-Rac by mass spectrometry (MS). No significant difference was observed between Rac and Rac coexpressed with VopC. Since a tranglutaminase reaction would add substantial mass, this result suggests that the reaction does not occur when these proteins are coexpressed (Figure S4). We analyzed chymotryptic digests of the two Rac samples using liquid chromatography followed by MS to determine whether Q61 had been modified. MS analysis demonstrated that only the deamidated form of Q61 was detected when Rac was coexpressed with VopC, while no deamidated form of Q61 was detected in the control sample, demonstrating that VopC activated Rac by deamidation of Q61 (Figure 3K, Figure S4, Table S3).

VopC-Mediated Bacterial Invasion Is Conserved in *V.cholerae* Strains

Some pathogenic *V. cholerae* non-O1 strains contain a T3SS2-like gene cluster encoding a similar repertoire of effectors, including VopC. Interestingly, two of these clinical isolates, *V. cholerae* 1587 and 623-39, in contrast to the well-studied *V. cholerae* serotypes O1 and O139, do not contain a cholera toxin, but are correlated with sporadic cholera epidemics, pathology in animal models, and limited, albeit unexplained cell invasion (Dalsgaard et al., 1995). Similar to *V. parahaemolyticus*, we observed cytotoxicity induced by *V. cholerae* 1587. Using time-course invasion experiments and LDH release assays, we obtained results that suggested that *V. cholerae* 1587 could replicate inside HeLa cells (Figures 4A–4C). We observed that *V. cholerae* 1587, but not the *V. cholerae* O1 El Tor strain, which contains cholera toxin but

not a T3SS, were able to invade nonphagocytic HeLa cells in a manner similar to that observed with *V. parahaemolyticus* (Figure 4D). Furthermore, *V. cholerae* 1587Δ*vopC* was no longer able to invade HeLa cells, and actin accumulation inhibitor cytochalasin D was able to block *V. cholerae* 1587 invasion, suggesting VopC has a similar role for invasion in *V. cholerae* as in *V. parahaemolyticus*. Thus, these *V. cholerae* non-O1 strains contain an active T3SS that mediates their invasion into host cells.

DISCUSSION

We have discovered that T3SS2 enables *V. parahaemolyticus* to act as an invasive pathogen. This T3SS2-mediated invasion is dependent on the presence of the effector VopC that has a deamidase/transglutaminase activity. Upon translocation into the host cell, VopC activates small GTPases Rac and CDC42 to induce changes in the actin cytoskeleton and facilitate the entry of *V. parahaemolyticus* into nonphagocytic host cells. It is possible that other known and unknown effectors secreted by T3SS2 may facilitate pathogen survival and replication inside the host cell, as well as cell lysis when a critical intracellular bacterial burden has been reached. Other known T3SS2 effectors include VopP/A, a Ser/Thr acetyltransferase; VopL/F, an actin nucleator; and VopV, an actin bundling protein (Hiyoshi et al., 2011; Liverman et al., 2007; Okada et al., 2010b; Trosky et al., 2007). We propose that these effectors are likely to be involved in the intracellular survival, replication, and spreading of these *Vibrio* species within the infected host. Although a direct connection between T3SS2-mediated invasion and T3SS2-mediated enterotoxicity has not been established, future studies will no doubt elucidate the molecular mechanisms of other yet-to-be-characterized T3SS2 effectors and how T3SS2 might contribute to possible intracellular pathogenesis.

Herein, we also observed that another pathogenic bacterium, a *V. cholerae* non-O1, non-O139 strain, contains a T3SS2 with a similar repertoire of effectors, including VopC. This strain of *V. cholerae* does not encode a cholera toxin but is involved in limited epidemic outbreaks (Dalsgaard et al., 1995). We propose that this pathogenicity for *V. cholerae* may be mediated by the recently acquired T3SS2 that allows for invasion. Our observations suggest that the *V. cholerae* T3SS2 functions independently of cholera toxin and could be sufficient for pathogenicity of *V. cholerae* during infection of its animal host.

Finally, the implications for invasive bacteria most likely extend beyond *Vibrio*, as there are other species of bacteria from marine environments that have acquired a T3SS encoding a VopC homolog (Table S1). These observations present another molecular paradigm for *Vibrio* pathogenicity, and future studies on invasion, survival, and spreading of the bacteria within the host will undoubtedly result in better understanding of signaling mechanisms used by both the host and the pathogen.

EXPERIMENTAL PROCEDURES

Bacterial Strains

V. parahaemolyticus CAB strains were derived from POR1 (RIMD 2210633 Δ*tdhAS*), generously provided by Drs. Tetsuya Iida and Takeshi Honda (Park et al., 2004b). They were created by deleting the transcription factors ExsA and/or VtrA that regulate the two T3SSs (Kodama et al., 2010; Kodama et al., 2007; Zhou et al., 2008). To induce T3SS2, media was supplemented with 0.05% bile salt and bacteria were grown at 37°C for 2 hr (Gotoh et al., 2010). *V. cholerae* strain 1587 was generously provided by Dr. John Mekalanos, and it was grown in LB at 37°C.

LDH Assays

LDH release at each indicated time point was measured in triplicate with the use of a Cytotoxicity Detection Kit (Takara) according to the manufacturer's instructions. Results are presented as cytotoxicity as calculated from percent of total lysis.

Invasion Assays

HeLa cells were infected at a multiplicity of infection (MOI) of 10 for the indicated time points. At each time point, 100 μg/ml gentamicin was added to kill extracellular bacteria. Cells were lysed with 0.5% Triton X-100 and the intracellular bacteria were assessed. For the gentamicin incubation experiments, cells were infected for 2 hr, washed with DMEM, and incubated in DMEM containing 100 μg/ml gentamicin. At each time point, cells were washed and lysed and the intracellular bacteria were assessed.

Electron Microscopy

HeLa cells were infected for 2 hr and fixed in 2.5% glutaraldehyde in 0.1M sodium cacodylate, followed by 1% osmium tetroxide in 0.1M sodium cacodylate. Cells were embedded in epoxy resin (Electron Microscopy Sciences) and polymerized at 60°C. Ultrathin sections were cut at 80 nm and stained with uranyl acetate and lead citrate. Sections were examined at 120 KV with a Tecnai G2 Spirit transmission electron microscope (FEI Company), and images were recorded on a Gatan USC1000 2k CCD camera (Gatan).

VopC Deletion Strain

The nucleotide sequences 1 kb upstream and 1 kb downstream of VopC were cloned into pDM4, a Cm^R OriR6K suicide plasmid (kindly provided by Dr. Doug Call). The resulting plasmid was conjugated into CAB2 and transconjugants were selected on media containing 25 μg/ml chloramphenicol. Bacteria were counterselected by growing on media containing 15% sucrose.

Reconstitution of CAB2Δ*vopC*

The Δ*vopC* deletion strain was reconstituted with the use of pBAD (Invitrogen) containing *vopC* FLAG or vopC C220S FLAG preceded by 1 kb of its upstream sequence and a kanamycin resistance gene.

Secretion Assay

pBAD *vopC*-FLAG or pBAD *vopC C220S*-FLAG were mated into different strains. Bacteria were induced with 0.05% bile salt at 37°C (Gotoh et al., 2010). Three hours after induction, the culture was centrifuged to separate supernatants and pellets. The supernatant was filtered and ice-cold trichloroacetate was added to a final concentration of 10%. Samples were kept on ice overnight and then centrifuged. The precipitates and pellets were analyzed by Western blotting with the use of a mouse anti-FLAG antibody (Sigma).

Tissue Culture and Transfection

HeLa cells were cultured in DMEM (Invitrogen) supplemented with 10% heat-inactivated fetal bovine serum (Sigma) at 37°C with 5% CO_2. Cells were transfected with the Fugene HD (Roche) transfection agent according to the manufacturer's protocol.

Confocal Microscopy

HeLa cells were fixed in 3.2% paraformaldehyde after treatment. Nuclei were stained with Hoechst (Sigma), and the actin cytoskeleton was stained with rhodamine-phalloidin (Molecular Probes). Cells were viewed on a Zeiss LSM 510 scanning confocal microscope, and images were converted with ImageJ and Adobe Photoshop.

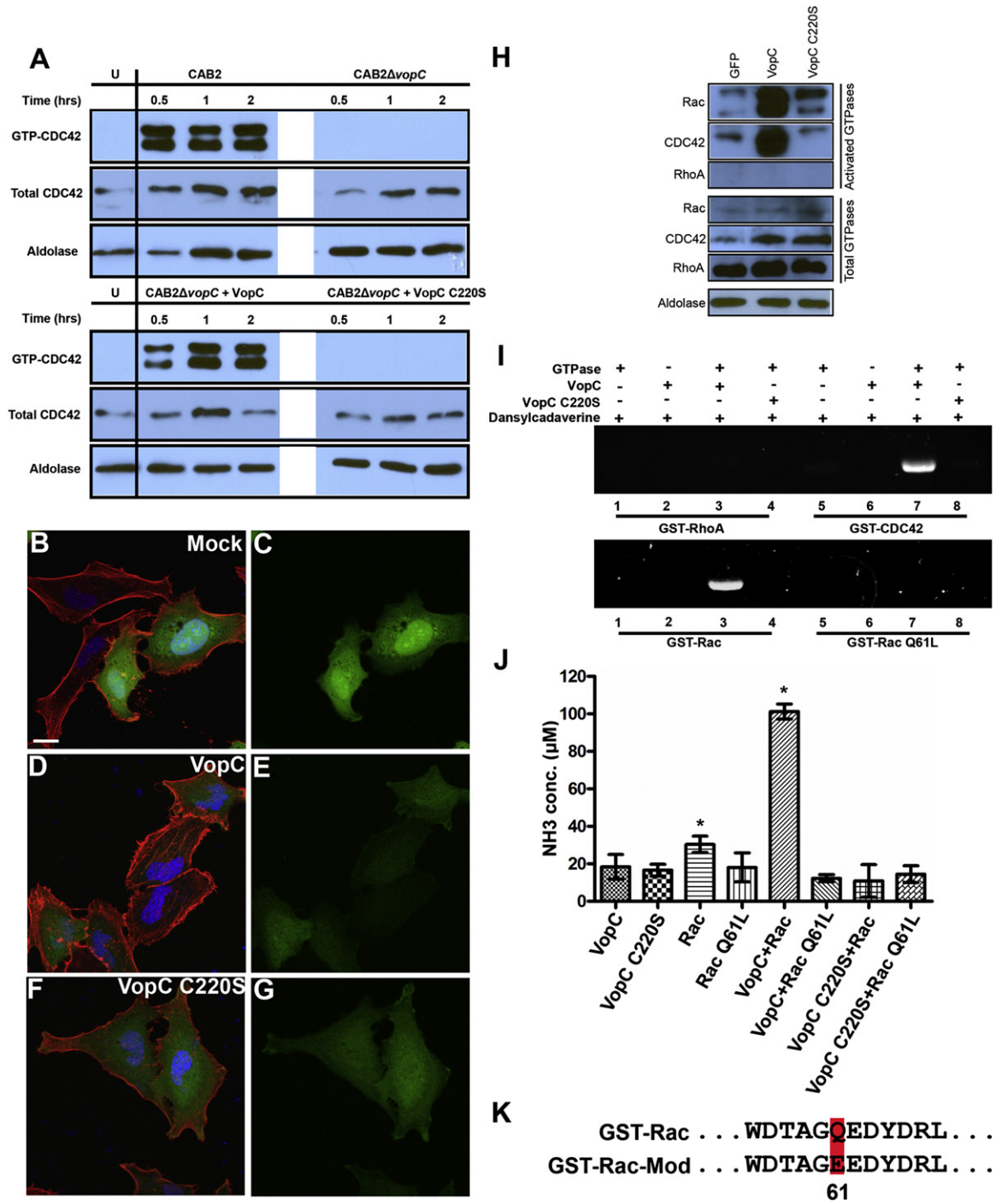

Figure 3. VopC Activates Rac and CDC42 by Deamidation of Glutamine 61

(A) HeLa cells infected with CAB2, CAB2Δ*vopC*, CAB2Δ*vopC* + VopC, or CAB2Δ*vopC* + VopC C220S and tested for active GTP-bound CDC42 with the use of GST-PAK PBD pull-down assays. For loading control, total cell lysates were immunoblotted with anti-aldolase.

(B–G) HeLa cells transfected with pSFFV-eGFP, pSFFV-GFP-VopCΔ67, or pSFFV-GFP-VopCΔ67 C220S. Cells were visualized by confocal microscopy with the use of GFP (green) to identify transfected cells. Nuclei were stained with Hoechst (blue), and actin cytoskeleton was stained with rhodamine-phalloidin (red). Scale bar represents 10μm.

(H) Transfected HeLa cells tested for active GTP-bound GTPases with the use of GST-PAK PBD (for Rac and CDC42) or GST-Rhotekin (for RhoA) pull-down assays. For loading control, total cell lysates were immunoblotted with anti-aldolase.

(I) MBP-VopCΔ67 or MBP-VopCΔ67 C220S incubated with GST-Rac, GST-CDC42, GST-RhoA, or GST-Rac Q61L in the presence of dansylcadaverine, followed by UV analysis.

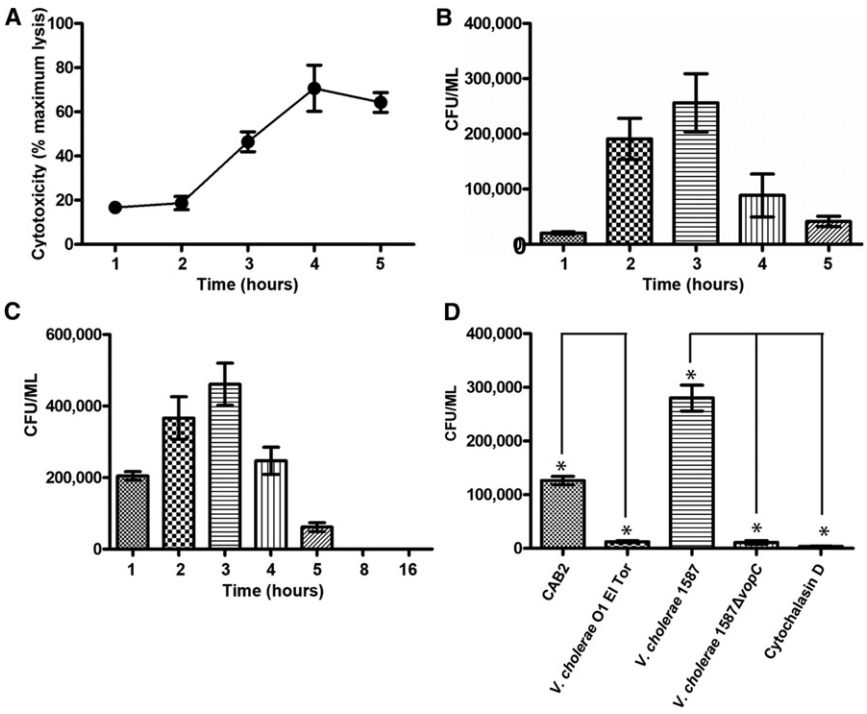

Figure 4. *V. cholerae* Non-O1 Strain Invades HeLa Cells

(A) HeLa cells infected with *V. cholerae* 1587 (closed circles). LDH release was evaluated as a measure of cytotoxicity. Error bars represent mean ± SD (n = 3).

(B) HeLa cells infected with *V. cholerae* 1587. Intracellular bacteria were assessed at indicated time points. Error bars represent mean ± SD (n = 3).

(C) HeLa cells infected with *V. cholerae* 1587 for 2 hr and incubated in medium containing gentamicin. The intracellular bacteria were determined at the indicated time points. Error bars represent mean ± SD (n = 3).

(D) HeLa cells infected with CAB2, *V. cholerae* O1 El Tor, 1587, 1587Δ*vopC*, or 1587 in the presence of cytochalasin D. After 2 hr of infection, intracellular bacteria were assessed. Error bars represent mean ± SD (n = 3). Asterisks indicate statistically significant differences between CAB2 and *V. cholerae* El Tor invasion, *V. cholerae* 1587 and 1587Δ*vopC* invasion, and *V. cholerae* 1587 invasion in the absence and presence of cytochalasin D (*$p < 0.0001$, n = 3; two-tailed t test).

GTPase Activation Assay in Infected and Transfected Cells

HeLa cells were infected at an MOI of 10. At each time point, cells were washed and lysates were collected by scraping into Mg^{2+} lysis buffer (20 mM Tris HCl [pH 7.5], 10 mM $MgCl_2$, 150 mM NaCl, 1% Triton X-100). Cellular debris was spun down at 12,000 × *g* for 20 min, and 500 μg of cleared lysates was added to 30 μg of GST-PAK PBD on glutathione agarose beads and incubated for 1 hr at 4°C. Samples were separated by SDS-PAGE and immunoblotted with anti-CDC42 (Cell Signaling). As a loading control, total cell lysates were immunoblotted with anti-aldolase (Santa Cruz Biotechnology). Transfected HeLa cells were collected and treated in a similar fashion as described above. Activated RhoA was pulled down with the use of a RhoA activation kit (Cytoskeleton) according to the manufacturer's instructions.

Recombinant Proteins

pGex-KG-PAK-PBD (provided by Dr. Neal Alto), pGex-KG-RhoA, pGex-KG-Rac, pGex-KG-Rac Q61L, pGex-KG-CDC42 (provided by Dr. Paul Sternweis), pET28a-MBP-VopCΔ67, and pET28a-MBP-VopCΔ67 C220S were transformed into BL21 (DE3) (Novagen). His-tagged proteins (MBP-VopCΔ67 and MBP-VopCΔ67 C220S) were purified with the use of Ni^{2+} affinity purification (QIAGEN). GST-tagged proteins (GST-PAK-PBD, GST-RhoA, GST-Rac, GST-Rac Q61L, and GST-CDC42) were purified with the use of glutathione agarose beads (Sigma).

Transglutaminase Assay

A total of 3 mg/ml of GST-RhoA, GST-Rac, GST-Rac Q61L, or GST-CDC42 was incubated with a 1:20 molar ratio of MBP-VopCΔ67 or MBP-VopCΔ67 C220S and 5 mM dansylcadaverine (Sigma) at 37°C for 2 hr. Samples were boiled and separated on 12% SDS-PAGE. Gels were examined with UV exposure through the use of an AlphaImager 2200 (Alpha Innotech Corporation), and images were recorded. Then, gels were stained with Coomassie Brilliant Blue (Biorad) for protein band observation.

Deamidation Assay

A total of 120 μM of GST-Rac or GST-Rac Q61L was incubated with a 1:20 molar ratio of MBP-VopCΔ67 or MBP-VopCΔ67 C220S at 37°C for 2 hr. The released NH_4^+ from glutamine deamidation was measured with the use of an ammonia assay kit (Sigma) according to the manufacturer's instructions.

MS

pGex-KG-Rac alone or pGex-KG-Rac and pET28a-MBP-VopCΔ67 together were transformed into BL21 (DE3) (Novagen) for protein expression. GST-Rac was purified with the use of glutathione agarose beads (Sigma). Proxeon nano-tips (Denmark) were used to inject the samples into a QStar XL Q-TOF mass spectrometer (Applied Biosystems). Spectra were acquired with a mass range of m/z 500–2,000. The molecular weights of proteins were calculated with the Bayesian Protein Reconstruct tool of the Analyst QS1.1 software.

Tandem MS

Ten micrograms of each sample were fractionated by SDS-PAGE, and bands containing GST-Rac were cut out, treated with DTT and iodoacetamide, and digested with chymotrypsin. Samples from the digests were analyzed by nano-LC/MS/MS through the use of a system in which a Dionex LC-Packings HPLC (Sunnyvale, CA) was coupled with an LTQ Orbitrap Velos (Thermo Scientific).

VopC Deletion in *V. cholerae* 1587

The *V. cholerae* 1587Δ*vopC* strain was generated essentially as described previously (Merriam et al., 1997; Walker and Miller, 2004). In brief, regions 1 kb upstream and downstream of VopC were cloned into pSR47S, a Kan^R OriR6K suicide plasmid (kindly provided by Dr. Virginia Miller). pSR47s was then conjugated into *V. cholerae* 1587 and transconjugants were selected by replating twice on *Vibrio*-selective medium (VSM) containing 60 μg/ml

(J) MBP-VopCΔ67 or MBP-VopCΔ67 C220S incubated with GST-Rac or GST-Rac Q61L and analyzed for release of ammonia. Statistically significant differences were shown between the ammonia release from GST-Rac incubated with VopC and GST-Rac alone ($p = 0.0036$, n = 3) with the use of a two-tailed t test. Error bars represent mean ± SD (n = 3).

(K) Alignment of the switch 2 region from Rac and VopC-modified Rac. The changed residue is highlighted in red.

kanamycin. Bacteria were counterselected by growing on media containing sucrose.

SUPPLEMENTAL INFORMATION

Supplemental Information includes four figures and three tables and can be found with this article online at doi:10.1016/j.celrep.2012.04.004.

LICENSING INFORMATION

ACKNOWLEDGMENTS

For insightful discussions, critical reading, and/or generous supply of reagents, we thank N. Alto, T. Iida, T. Honda, L. McCarter, M. Phillips, V. Miller, J. Mekalanos, and the Orth lab. K.O., L.Z., C.A.B., and A.M.K. are supported by grants from NIH and the Welch Foundation (I-1561). K.O. is a Beckman Young Investigator, Burroughs Wellcome Investigator, and W.W. Caruth Biomedical Scholar.

Received: February 16, 2012
Revised: March 26, 2012
Accepted: April 17, 2012
Published online: May 3, 2012

REFERENCES

Akeda, Y., Nagayama, K., Yamamoto, K., and Honda, T. (1997). Invasive phenotype of Vibrio parahaemolyticus. J. Infect. Dis. *176*, 822–824.

Aktories, K., and Barbieri, J.T. (2005). Bacterial cytotoxins: targeting eukaryotic switches. Nat. Rev. Microbiol. *3*, 397–410.

Broberg, C.A., and Orth, K. (2010). Tipping the balance by manipulating post-translational modifications. Curr. Opin. Microbiol. *13*, 34–40.

Broberg, C.A., Calder, T.J., and Orth, K. (2011). Vibrio parahaemolyticus cell biology and pathogenicity determinants. Microbes Infect. *13*, 992–1001.

Dalsgaard, A., Albert, M.J., Taylor, D.N., Shimada, T., Meza, R., Serichantalergs, O., and Echeverria, P. (1995). Characterization of Vibrio cgolerae non-O1 serogroups obtained from an outbreak of diarrhea in Lima, Peru. J. Clin. Microbiol. *33*, 2715–2722.

Doye, A., Mettouchi, A., Bossis, G., Clément, R., Buisson-Touati, C., Flatau, G., Gagnoux, L., Piechaczyk, M., Boquet, P., and Lemichez, E. (2002). CNF1 exploits the ubiquitin-proteasome machinery to restrict Rho GTPase activation for bacterial host cell invasion. Cell *111*, 553–564.

Flatau, G., Lemichez, E., Gauthier, M., Chardin, P., Paris, S., Fiorentini, C., and Boquet, P. (1997). Toxin-induced activation of the G protein p21 Rho by deamidation of glutamine. Nature *387*, 729–733.

Gotoh, K., Kodama, T., Hiyoshi, H., Izutsu, K., Park, K.S., Dryselius, R., Akeda, Y., Honda, T., and Iida, T. (2010). Bile acid-induced virulence gene expression of Vibrio parahaemolyticus reveals a novel therapeutic potential for bile acid sequestrants. PLoS ONE *5*, e13365.

Ham, H., Sreelatha, A., and Orth, K. (2011). Manipulation of host membranes by bacterial effectors. Nat. Rev. Microbiol. *9*, 635–646.

Hiyoshi, H., Kodama, T., Saito, K., Gotoh, K., Matsuda, S., Akeda, Y., Honda, T., and Iida, T. (2011). VopV, an F-actin-binding type III secretion effector, is required for Vibrio parahaemolyticus-induced enterotoxicity. Cell Host Microbe *10*, 401–409.

Horiguchi, Y. (2001). Escherichia coli cytotoxic necrotizing factors and Bordetella dermonecrotic toxin: the dermonecrosis-inducing toxins activating Rho small GTPases. Toxicon *39*, 1619–1627.

Kodama, T., Rokuda, M., Park, K.S., Cantarelli, V.V., Matsuda, S., Iida, T., and Honda, T. (2007). Identification and characterization of VopT, a novel ADP-ribosyltransferase effector protein secreted via the Vibrio parahaemolyticus type III secretion system 2. Cell Microbiol. *9*, 2598–2609.

Kodama, T., Gotoh, K., Hiyoshi, H., Morita, M., Izutsu, K., Akeda, Y., Park, K.S., Cantarelli, V.V., Dryselius, R., Iida, T., and Honda, T. (2010). Two regulators of Vibrio parahaemolyticus play important roles in enterotoxicity by controlling the expression of genes in the Vp-PAI region. PLoS ONE *5*, e8678.

Liverman, A.D., Cheng, H.C., Trosky, J.E., Leung, D.W., Yarbrough, M.L., Burdette, D.L., Rosen, M.K., and Orth, K. (2007). Arp2/3-independent assembly of actin by Vibrio type III effector VopL. Proc. Natl. Acad. Sci. USA *104*, 17117–17122.

Makino, K., Oshima, K., Kurokawa, K., Yokoyama, K., Uda, T., Tagomori, K., Iijima, Y., Najima, M., Nakano, M., Yamashita, A., et al. (2003). Genome sequence of Vibrio parahaemolyticus: a pathogenic mechanism distinct from that of V cholerae. Lancet *361*, 743–749.

Masuda, M., Betancourt, L., Matsuzawa, T., Kashimoto, T., Takao, T., Shimonishi, Y., and Horiguchi, Y. (2000). Activation of rho through a cross-link with polyamines catalyzed by Bordetella dermonecrotizing toxin. EMBO J. *19*, 521–530.

Merriam, J.J., Mathur, R., Maxfield-Boumil, R., and Isberg, R.R. (1997). Analysis of the Legionella pneumophila flil gene: intracellular growth of a defined mutant defective for flagellum biosynthesis. Infect. Immun. *65*, 2497–2501.

Nishibuchi, M., and Kaper, J.B. (1995). Thermostable direct hemolysin gene of Vibrio parahaemolyticus: a virulence gene acquired by a marine bacterium. Infect. Immun. *63*, 2093–2099.

Okada, N., Iida, T., Park, K.S., Goto, N., Yasunaga, T., Hiyoshi, H., Matsuda, S., Kodama, T., and Honda, T. (2009). Identification and characterization of a novel type III secretion system in trh-positive Vibrio parahaemolyticus strain TH3996 reveal genetic lineage and diversity of pathogenic machinery beyond the species level. Infect. Immun. *77*, 904–913.

Okada, K., Chantaroj, S., Taniguchi, T., Suzuki, Y., Roobthaisong, A., Puiprom, O., Honda, T., and Sawanpanyalert, P. (2010a). A rapid, simple, and sensitive loop-mediated isothermal amplification method to detect toxigenic Vibrio cholerae in rectal swab samples. Diagn. Microbiol. Infect. Dis. *66*, 135–139.

Okada, N., Matsuda, S., Matsuyama, J., Park, K.S., de los Reyes, C., Kogure, K., Honda, T., and Iida, T. (2010b). Presence of genes for type III secretion system 2 in Vibrio mimicus strains. BMC Microbiol. *10*, 302.

Park, K.-S., Ono, T., Rokuda, M., Jang, M.-H., Okada, K., Iida, T., and Honda, T. (2004a). Functional characterization of two type III secretion systems of Vibrio parahaemolyticus. Infect. Immun. *72*, 6659–6665.

Park, K.S., Ono, T., Rokuda, M., Jang, M.H., Iida, T., and Honda, T. (2004b). Cytotoxicity and enterotoxicity of the thermostable direct hemolysin-deletion mutants of Vibrio parahaemolyticus. Microbiol. Immunol. *48*, 313–318.

Schmidt, G., Sehr, P., Wilm, M., Selzer, J., Mann, M., and Aktories, K. (1997). Gln 63 of Rho is deamidated by Escherichia coli cytotoxic necrotizing factor-1. Nature *387*, 725–729.

Trosky, J.E., Li, Y., Mukherjee, S., Keitany, G., Ball, H., and Orth, K. (2007). VopA inhibits ATP binding by acetylating the catalytic loop of MAPK kinases. J. Biol. Chem. *282*, 34299–34305.

Walker, K.A., and Miller, V.L. (2004). Regulation of the Ysa type III secretion system of Yersinia enterocolitica by YsaE/SycB and YsrS/YsrR. J. Bacteriol. *186*, 4056–4066.

Zhou, X., Shah, D.H., Konkel, M.E., and Call, D.R. (2008). Type III secretion system 1 genes in Vibrio parahaemolyticus are positively regulated by ExsA and negatively regulated by ExsD. Mol. Microbiol. *69*, 747–764.